# Inverse Hybrid Modelling of Virtual Microstructure for Knowledge Management in Materials Characterisation

M.F. Abbod, D.A. Linkens, C.M. Sellars* and M. Mahfouf

IMMPETUS
Department of Automatic Control and Systems Engineering
* Department of Engineering Materials
University of Sheffield, Sheffield, UK
Phone: +44-114-2225612, FAX: +44-114-2225661
Email: M.F.Abbod@sheffield.ac.uk

*Abstract* - **An inverse method is developed in order to estimate virtual variables (internal microstructure) of a material from compression tests. The direct model used to simulate mechanical properties of the materials is a hybrid type which consists of physical and data driven (neuro-fuzzy) components. It predicts the material properties and internal microstructure during hot deformation. For compression and temperature treatments, any model output of a mechanical test can be computed and compared with experimental data. A Gauss-Newton algorithm is implemented to solve the least-squares algorithms associated with the inverse problem. The optimisation module is coupled with semi-analytical sensitivity analysis. The technique developed will facilitate the design of optimal experimentation for model refinement and knowledge management.**

*Keywords* - Parameter estimation, semi–physical model, neuro-fuzzy models, confidence intervals, mechanical tests, knowledge management.

## I. INTRODUCTION

Numerical simulation of metal-forming processes requires internal microstructural data such as the subgrain size and orientation. Therefore, the identification of these parameters is crucial. This paper describes a method which is able to determine the parameters of a physical model taking into account the evolution of the deformation forces and the temperature during a mechanical test involving moderate strain. Empirical mechanical parameter estimation techniques from laboratory tests are based on simple analytical models assuming that the material microstructure has linear behaviour. When the internal microstructure is altered during a mechanical test, these empirical techniques cannot be used. The inverse analysis approach consists of coupling a direct physical model with an optimisation module allowing the simultaneous and automatic identification of the whole parameter set in the physical equations. Optimisation methods are generally based on zero-order methods (genetic algorithms [6], simplex methods [9] or gradient methods [3]. The computation of the cost function gradient can be done using an analytical method [5], a finite difference method or a semi-analytical method [10, 7].

In this work, an inverse analysis technique based on a hybrid model comprising both physical and neuro-fuzzy components is used for the identification of the microstructure variables from test measurements. The identification is based on such a hybrid model developed for aluminium alloys and extended to steel materials. The inverse model obtained via the minimisation of an objective function representative of the difference between the experimental information (deformation conditions, temperature, grain size and recrystallisation time) and the corresponding computed values, formulated in a least squares sense. The optimisation procedure is based on a Gauss-Newton algorithm utilising an accurate computation of the sensitivity matrix. Validation of the proposed approach was first done using an experimental data-base, and then extended to unseen data from the literature. A literature database has been compiled which contains all the information gathered during the research project. This will facilitate knowledge management for researchers in the future, as well as giving insight information as to where the data came from, and how dense it is for certain process conditions which impacts on the confidence in the prediction for particular conditions.

## II. DIRECT MODEL

A powerful approach for generic modelling of material properties is one which includes the internal states of the process as well as the inputs and outputs. The output variables are the flow stress ($\sigma$), the density of nuclei for recrystallisation ($N_v$) and the average growth rate for recrystallisation ($\overline{G}$) in terms of the state variables, while the values for the input variables are strain rate ($\dot{\varepsilon}$) and temperature (T) [11].

In thermomechanical processing, the strain rate and temperature (which can be described by the Zener-Hollomon parameter $Z = \dot{\varepsilon}\exp(Q/RT)$, where Q is the activation energy) generally change continuously during the deformation process itself and may change from one rolling pass to another.

Modelling of the flow stress is carried out in terms of the internal state variables represented by as the dislocation density, subgrain size and misorientation ($\rho_i^{-1/2}$, $\delta$, $\theta$) which in turn are determined by the deformation conditions (T, $\dot{\varepsilon}$, $\varepsilon$). The final stress is the sum of the effective stress ($\sigma_e$) and the internal stress ($\sigma_i$) that arises from the dislocation structure [12]. Thus,

$$\begin{aligned} \sigma &= \sigma_e + \sigma_i \\ \sigma_i &= \sigma_{\rho i} + \sigma_\delta + \sigma_f \\ \sigma_{\rho i} &= \alpha_1 MGb\rho^{1/2} \\ \sigma_\delta &= \alpha_2 MGb/\delta \end{aligned} \qquad (1)$$

where $\sigma_{pi}$ is the thermal stress due to interaction of dislocation inside the subgrain, $\sigma_\delta$ is the long range internal back stress due to subgrain boundaries, $\sigma_d$ is the stress arising from grain boundaries, and $\sigma_p$ is the stress due to second phase particles.

The overall model is based on the evolution of microstructure in a thermomechanical environment. It includes modelling the mechanics and heat transfer conditions to provide input data for the microstructural model as shown in Fig. 1. The model must involve microstructure/property relationships that are used interactively to compute the product properties. It should also allow for examination of the internal variables examination and optimisation of the process conditions within the constraints imposed by the plant.

Nucleation of recrystallisation takes place in different places within a deformed material. A generalised model to describe the effect of subgrain size distribution across grain boundaries or other mobile boundaries has been proposed recently [13] and is described by the following equation:

$$N_V = p_1\lambda_1 P_V + p_2\lambda_2 \frac{L_V}{\bar{\delta}} + p_3\lambda_3 \frac{S_V}{\bar{\delta}^2} + p_4\lambda_4 + \frac{P_\theta}{\bar{\delta}^3} \quad (2)$$

where $S_v$ = *(0.49 exp(-strain/1.155) + exp(strain/1.155) + 0.571)/do* , $P_v$ is the number of grain corners per unit volume, and $L_v$ is the line length per unit volume.

As the strain regime covers a wide range of thermomechanical processing conditions, the equation can be simplified by assuming $p_3$ is constant for all strains used in the calculations [13]:

$$N_V \approx p_3\lambda_3 \frac{S_V}{\bar{\delta}^2} \quad (3)$$

where $d_0$ is the grain diameter, $\lambda_3$ is a material dependent constant, and $p_3$ is a probability term.

Recrystallisation kinetics is determined by both nucleation density and growth rate of nuclei. If the nucleation is site-saturated, which is a reasonable approximation after hot deformation, then the following kinetics law of recrystallisation is obtained:

$$X(t) = 1 - exp(X_{ext}(t)) \quad (4)$$

where $X(t)$ is the fraction recrystallised after annealing time $t$ and $X_{ext}(t)$ is the corresponding extended volume which is determined by:

$$X_{ext}(t) = \frac{3}{4}\pi N_V (G.t)^3 \quad (5)$$

where $G$ is the growth rate of the recrystallisation nuclei which is mainly affected by the recovery from the deformed microstructure and the spatial distribution of the stored energy on the scale of the grain size and is related to the stored energy $P_D$ by:

$$G = M_{gb} P_D \quad (6)$$

where $M_{gb}$ is the grain boundary mobility.

The stored energy is calculated by:

$$P_D = \frac{Gb^2}{10}\left[\rho_i(1-\ln(10b\rho_i^{1/2})) + \frac{2\theta}{b\delta}(1+\ln(\frac{\theta_c}{\theta}))\right] \quad (7)$$

where $\theta_c$ is the critical angle for distinguishing between a grain and subgrain boundary (approximately 15 degree).

The time for 50% recrystallisation can be calculated by the following equation:

$$t_{50} = C_3 P_D^{-1} N_V^{-1/3} \quad (8)$$

where $C_3$ is a temperature-dependent material constant.

For site-saturated nucleation, the recrystallised grain size is simply calculated from the nucleation density as:

$$d_{rex} = A\, N_V^{-1/3} \quad (9)$$

where $A$ is a geometric parameter to relate the surface linear intercept size and spatial diameter of the grains. For a grain structure of uniform tetrakiadecahedra (TKD), $A$ = 0.2347.

## III. INVERSE MODELLING

The main idea of the inverse method is to fit a mathematical model to a set of experimentally obtained data. The model depends on a set of $N$ design parameters $x_k$ where $k = 1, \ldots, N$. An objective function $f(x_k)$ is defined, giving the error between the model approximation and the set of experimental data. The objective function is designed using a least-squares formulation such that best-fit design parameters are obtained by its minimisation.

The inverse modelling concept is based on predicting the material internal states, where the input/output deformation conditions and material characteristics are available (Fig. 2). Based on the developed physical component for the single-phase material, the selected material under test was modelled using the combined physical equations and neuro-fuzzy models [1]. In designing the experimental test conditions, the process input variables are selected, such as the temperature, strain, and strain-rate as well as the chemical composition of the material which should be known before performing the test. The final material characteristics, such as the stress and the recrystalisation kinetics can be measured at the end of the test. The developed physical model can then be used to predict the internal states of the material and correct the model parameters based on an optimisation procedure and some measured variables of the internal states.

Table 1 shows the parameters of the physical equation governing the recrystallisation kinetics. The listed parameters are based on the developed physical model for Al-1%Mg material [13]. The first stage in the inverse modelling was to validate the methodology on the existing data that are used to develop the model. Table 2 shows the experimental and predicted internal states based on the hybrid modelling technique and the inverse technique. The results are shown graphically in Fig. 3. At a strain of 1 both the subgrain size and misorientation were under-predicted which is due to errors in the experimental measurements.

The next stage was to verify the model on data which have not been used in developing the model. Furu et al [4] used the same material and deformation conditions in mechanical tests. Not many data were available for the internal states. Table 3 shows the prediction results for the internal states using the hybrid and the inverse modelling technique.

In order to validate the technique for different materials and deformation conditions, Cotner and Tegart [2] provide some results on Al-1%Mg material deformed at different temperature and 2.83 /s strain rate. However, not all the

internal states were available (only the subgrain size and misorientation) while only the time for 50% recrystalisation was measured plus the flow stress. In order to implement the same concept, it was not possible to perform the same exercise since the $d_{rex}$ measurements are not available. Furthermore, some measurements were made at 0.73 strain while the other were made at 2.35. The data were used with the same physical equations parameters while the prediction was the dislocation density, the $d_{rex}$ at two strains and the subgrain misorientation at 0.73 strain (Table 4). The results in these tables show the technique to be flexible in terms of predicting the unmeasured variables and hence allows for designing the experiments based on the prediction of the inverse model.

TABLE 1: Parameters for physical equations.

| parameter | value |
|---|---|
| Burger vector (b) | 2.86E-10 |
| shear modulus (G) | 1.97E+10 |
| p3 | 0.0191 |
| λ3 | 0.692 |
| C | 7.0E+10 |
| M | 3.0000 |
| A | 3.2860 |
| α1 | 0.3800 |
| α2 | 0.7900 |

TABLE 2: Training data for Al-1%Mg at 385°C and 2.5 strain rate [13].

| strain | model type | ρ (1/m²) | δ (μm) | θ (°) |
|---|---|---|---|---|
| 0.4 | experimental | 1.40E+13 | 1.57 | 1.48 |
| | hybrid model | 1.50E+13 | 1.58 | 1.65 |
| | inverse model | 1.20E+13 | 1.57 | 1.49 |
| 0.7 | experimental | 2.40E+13 | 1.45 | 2.54 |
| | hybrid model | 1.70E+13 | 1.42 | 2.31 |
| | inverse model | 1.69E+13 | 1.45 | 2.53 |
| 1.0 | experimental | 1.70E+13 | 1.5 | 3.9 |
| | hybrid model | 1.79E+13 | 1.47 | 3.53 |
| | inverse model | 1.83E+13 | 1.44 | 3.50 |
| 1.3 | experimental | 1.80E+13 | 1.61 | 3.6 |
| | hybrid model | 1.43E+13 | 1.28 | 2.44 |
| | inverse model | 1.84E+13 | 1.45 | 3.53 |

TABLE 3: Testing data for Al-1%Mg at 385°C and 2.5 $s^{-1}$ strain rate [4].

| strain | model type | ρ (1/m²) | δ (μm) | θ (°) |
|---|---|---|---|---|
| 0.4 | experimental | 1.80E+13 | 1.57 | 1.50 |
| | hybrid model | 1.49E+13 | 1.58 | 1.57 |
| | inverse model | 1.20E+13 | 1.48 | 1.49 |
| 1.0 | experimental | 1.70E+13 | 1.50 | 3.90 |
| | hybrid model | 1.77E+13 | 1.46 | 1.44 |
| | inverse model | 1.83E+13 | 3.86 | 3.50 |

## IV. INVERSE MODELLING WITH PARAMETERS ESTIMATION

The necessary experimental testing mainly involves hot rolling and subsequent resource-intensive metallographic examination with some supplementary plane strain compression testing. Such experimental work has been

TABLE 4: Testing data for Al-1%Mg at 2.35 strain and 2.83 /s strain rate [2].

| | temp (°C) | 400 | 450 | 500 | 550 |
|---|---|---|---|---|---|
| exp | θ (°) | 2.20 | 2.30 | 2.40 | 2.50 |
| | δ (μm) | 7.40 | 9.20 | 10.20 | 11.60 |
| | $T_{50}$ (sec) | 410 | - | 22 | 7 |
| | σ (MPa) | 12.00 | 9.60 | 7.00 | 5.10 |
| pred | ρ (1/m²) | 3.9E10 | 2.5E10 | 2.4E10 | 2.1E10 |
| | θ (°)* | 1.00 | 0.81 | 0.66 | 0.55 |
| | $d_{rex}$ (μm) | 74.18 | 85.76 | 91.87 | 100.10 |
| | $d_{rex}$ (μm)* | 107.62 | 124.43 | 133.29 | 145.22 |

* @ 0.73 strain

conducted using samples of two similar alloys of commercial purity steel Fe3%Si under compression testing. The materials had the compositions shown in Table 5 and they have the same metallurgical recrystallisation kinetics as for the aluminium alloys. Experimental results together with the deformation conditions were fed to the inverse modelling technique along with the optimisation technique.

The optimiser was used to search for the best-fit parameters which optimise the physical equations in order to calculate the internal states using the recrystallisation experimental data. These five parameters were optimised using a least squares error function. The results of the optimised parameters for the physical equations, as well as the constants, are displayed in Table 6.

TABLE 5: Chemical composition of the two Fe3%Si materials.

| C | S | Si | P | Mn | Ni | Cu | Cr | Mo | Al |
|---|---|---|---|---|---|---|---|---|---|
| 0.036 | 0.019 | 3.16 | 0.004 | 0.089 | 0.011 | 0.018 | 0.008 | 0.002 | 0.003 |
| 0.016 | 0.004 | 3.31 | <0.005 | 0.13 | <0.002 | <0.02 | <0.002 | <0.02 | 0.023 |

TABLE 6: Results of parameters estimation.

| parameter | value |
|---|---|
| Burgers vector (b) | 3E10 |
| shear modulus (G) | 5E10 |
| p3 | 0.02955 |
| λ3 | 0.692 |
| C | 20.5 |
| M | 3.1 |
| A | 3.2860 |
| α1 | 0.38 |
| α2 | 0.79 |

## V. SENSITIVITY ANALYSIS

The aim of sensitivity analysis was to estimate the rate of change in the output of a model with respect to changes in model parameters. Such knowledge is important for (a) evaluating the applicability of the model, (b) determining parameters for which it is important to have more accurate values, and (c) understanding the behaviour of the system being modelled. The choice of a sensitivity analysis method depends to a great extent on (a) the sensitivity measure employed, (b) the desired accuracy in the estimates of the sensitivity measure, and (c) the computational cost involved.

Based on the choice of a sensitivity metric and the variation in the model parameters, sensitivity analysis methods can be broadly classified into the following categories:

- *Sampled variation of parameters or model formulation:* In this approach, the model is run at a set of sample points (different combinations of parameters of concern) or with straightforward changes in model structure (e.g., in model resolution). Sensitivity measures that are appropriate for this type of analysis include the response from arbitrary parameter variation, normalized response and extrema.
- *Domain-wide sensitivity analysis:* Here, the sensitivity involves the study of the system behaviour over the entire range of parameter variation, often taking the uncertainty in the parameter estimates into account.
- *Local sensitivity analysis:* Here, the focus is on estimates of model sensitivity to input and parameter variation in the vicinity of a sample point. This sensitivity is often characterized through gradients or partial derivatives at the sample point.

Sensitivity testing involves studying model responses for a set of changes in model formulation, and for selected model parameter combinations. Analytical methods involve either the differentiation of model equations and subsequent solution of a set of auxiliary sensitivity equations, or the reformulation of the original model using stochastic algebraic/differential equations. On the other hand, the sampling-based methods involve running the original model for a set of input/parameter combinations (sample points) and estimating the sensitivity/uncertainty using the model outputs at those points.

In this work, the sampling method has been implemented by changing the model parameters as well as the inputs within defined ranges. The output error bands were generated by using Monte Carlo simulation via selecting random parameters variation within 10% of each parameter. The probabilistic parameters in the physical equations were *p3* and *A*. The simulation has been done to obtain the sensitivity of the three internal states. The effect of the parameters variation on $d_{rex}$ and t50 is shown in Fig. 4. It is seen that $d_{rex}$ is almost constant with respect to changing $\rho$ and $\theta$ (Fig. 4-b,f), and has constant confidence bands. The sensitivity of $d_{rex}$ with respect to $\delta$ shows a small increase in the confidence bands as $\delta$ increases (Fig. 4-d). On the other hand, $t_{50}$ shows narrow confidence bands with respect to changes in $\rho$, $\delta$, and $\theta$ (Fig. 4-a,c,e). The conclusion from the sensitivity analysis is that the system is not sensitive to $\rho$, it is sensitive to $\delta$, while only $t_{50}$ is sensitive and $\theta$.

## VI. CONCLUSION

An inverse method coupled with a semi-analytical sensitivity module is presented and validated in this paper. It is shown that the semi-analytical method is stable and relatively fast. Moreover, it makes it easy to change the constitutive law because it only uses terms calculated from the direct model. It has been shown also that an important correlation between two sensitivity vectors can make the estimation ill-posed i.e. the cost function has 'valleys', while confidence intervals at the end ranges of the estimation can be wide. On the other hand, the inverse method makes possible an efficient fitting of experimental data based on computed data.

The developed modelling technique has been validated against different experimental results in materials testing under different deformation conditions from different research groups. The developed model can be used by both the research community and industry as it provides the internal state variables as well as the final material properties. Furthermore, the model can be used to predict the internal state variables which are difficult, expensive and time consuming to measure. The model has been linked to a knowledge base that describes the sources of the data as well as the operating range [14]. This will give the model a "confidence band" to which the prediction is attached.

Following further validation, the inverse model could be used to predict the "virtual" microstructure of materials under different deformation conditions and alloying content. Such prediction could then adaptively guide new experiments to further characterise the material structures and properties.

## VII. ACKNOWLEDGMENT

The authors are grateful to the UK Engineering and Physical Sciences Research Council for financial support for this research under grant number GR/L 50198.

## VIII. REFERENCES

[1] M.F. Abbod, D.A. Linkens and Q. Zhu, "Semi-physical modelling of internal states for aluminium alloys". *Materials Science and Technology*, Vol. A333, 2002, pp. 397-408.

[2] J.R. Cotner and WJ McG. Tegart, "High temperature deformation of aluminium-magnesium alloys at high strain rates", *Journal of the Institute of Metals*, Vol. 97, 1969, pp. 73-79.

[3] T.G. Faurholdt, "Inverse modelling of constitutive parameters for elastoplastic problems", *Journal of strain analysis,* Vol. 35, no. 6, 2000, p. 471.

[4] T. Furu, HR Shercliff, G.J. Baxter and C.M. Sellars, "The influence of transient deformation conditions on recrystallisation during thermomechanical processing of an Al-1% Mg alloy", *Acta Mater.*, Vol. 47, 1999, pp. 2377-2389.

[5] Gavrus, E. Massoni and J.L. Chenot, "The theological parameter identification formulated as an inverse finite element problem", *Inverse Problem in Engineering*, Vol. 7, 1999, pp.1-41.

[6] O. Ghouati and J.C. Gelin, "Gradient based methods, genetic algorithms and the finite element method for the identification of material parameters", *Simulation of Material Processing: Theory, Methods and Applications,* Huétink & Baaijens, 1998, pp.157-162.

[7] E. Massoni, B. Boyer and R. Forestier, "Inverse Analysis of thermomechanical upsetting tests using gradient method with semi-analytical derivatives, *Int. Journal of Thermal Sciences*, Vol. 41, no. 6, 2002, pp. 557-563.

[8] G.J. McRae, J.W. Tilden, and J.H. Seinfeld. "Global sensitivity analysis - a computational implementation

of the fourier amplitude sensitivity test (FAST)". *Computers and Chemical Engineering,* Vol. 6, no. 1, 1982, pp. 15-25.

[9] M. Pietrzyk, "Identification of parameters in the history dependent constitutive model of steels", *Annals of the CIRP*, Vol. 50, no. 1, 2001, pp.161-164.

[10] J.E. Scheuing, D.A. Tortorelli, "Inverse heat conduction problem solutions via second-order design sensitivities and Newton's method", *Inverse Problem in Engineering,* Vol 2, 1996, pp.227-262.

[11] C.M. Sellars, "Microstructure modelling in hot deformation", presented at Thermomechanical Processing: *Theory, Modelling, Practice [TMP2]*, Stockholm, Sweden, 1996a.

[12] C.M. Sellars, "Effect of varying hot deformation conditions on deformed microstructures and subsequent static recrystallization", in *3rd Int. Conf. on Recrystallization and Related Topics*, Monterey, California, USA, 1996b.

[13] C.M. Sellars and Q. Zhu, "Microstructural modelling of aluminium alloys during thermomechanical processing", *Materials Science and Engineering,* Vol. A280, 2000, pp. 1-7.

[14] C.M. Sellars, M.F. Abbod, Q. Zhu and D.A. Linkens, "Hybrid modelling methodology applied to microstrucural evolution during hot deformation of aluminium alloys" in *THERMEC'03*, Madrid, Spain, 7-11 July 2003 (keynote paper), pp. 27-34.

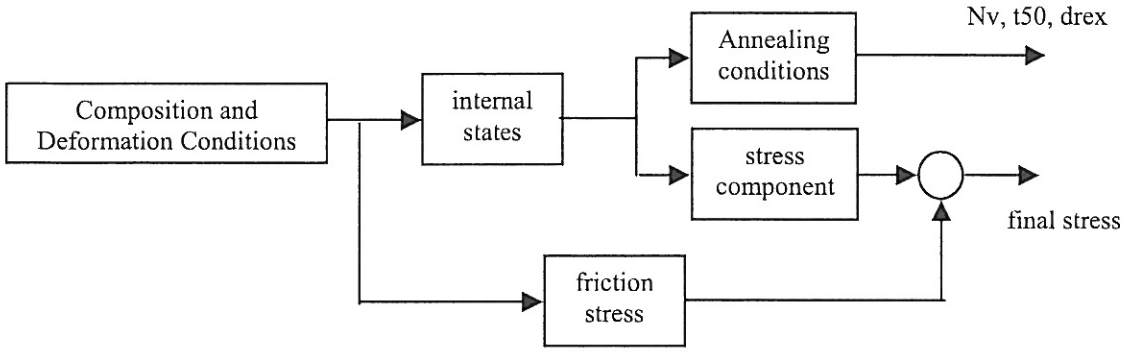


Fig. 1. Block diagram of the microstructure base model.

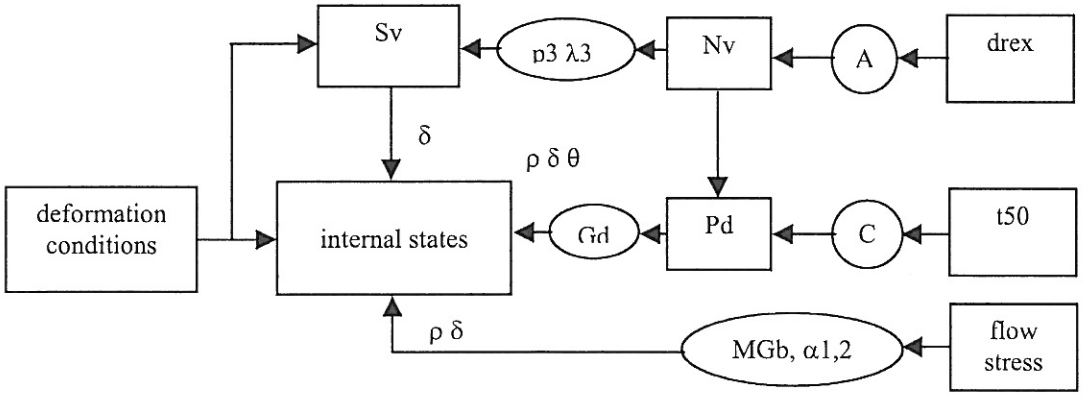


Fig. 2. Block diagram of the inverse model.

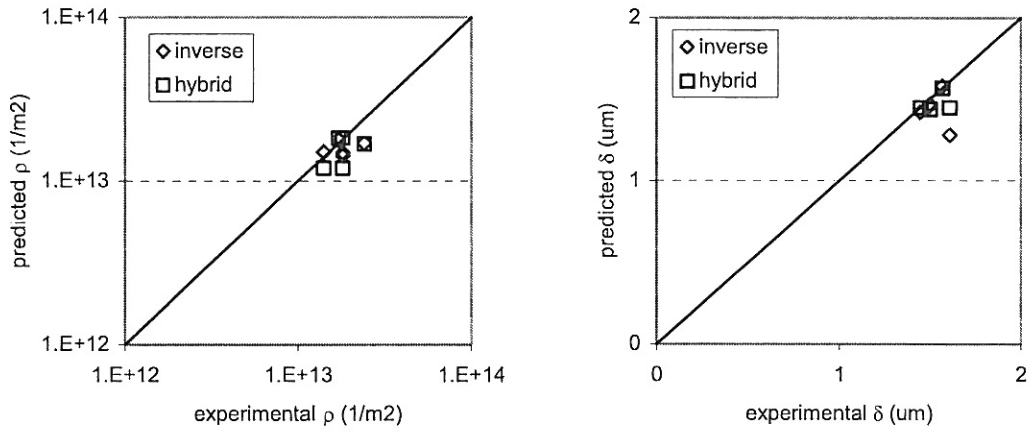


(a) dislocation density

(b) subgrain size

Fig. 3. Experimental versus predicted internal states using the inverse and the hybrid model techniques.

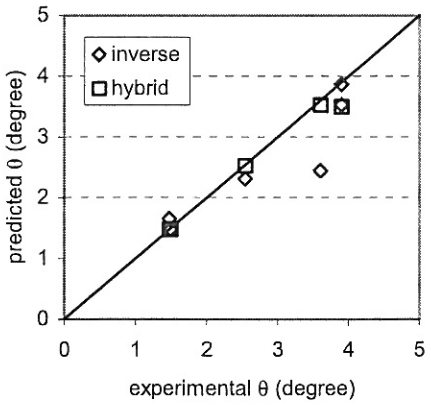


(c) subgrain misorientations

Fig. 3. Experimental versus predicted internal states using the inverse and the hybrid model techniques.

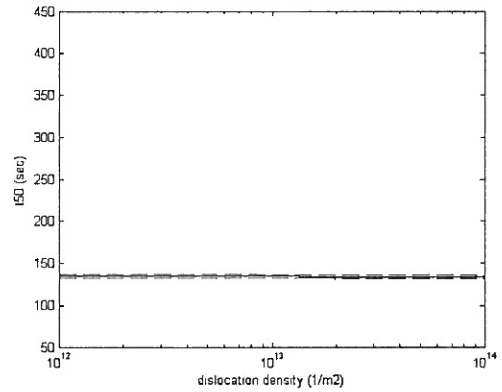


(a) $t_{50}$ sensitivity with respect to ρ

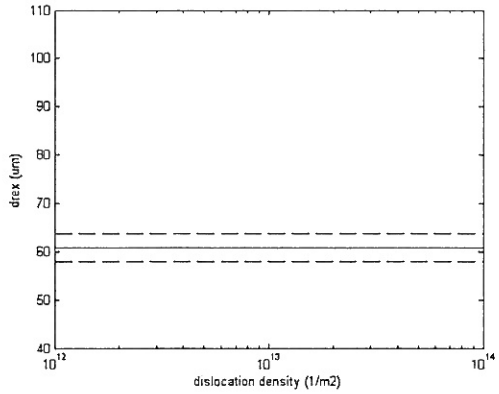


(b) $d_{rex}$ sensitivity with respect to ρ

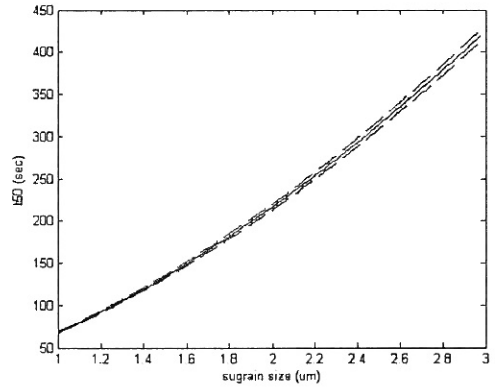


(c) $t_{50}$ sensitivity with respect to δ

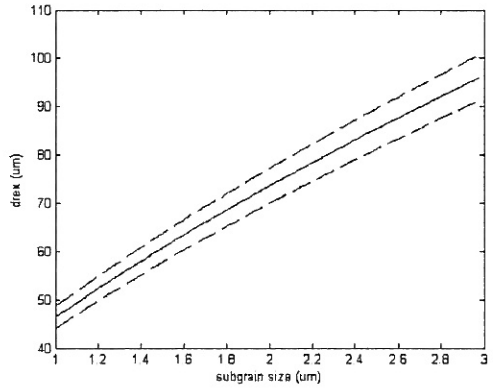


(d) $d_{rex}$ sensitivity with respect to δ

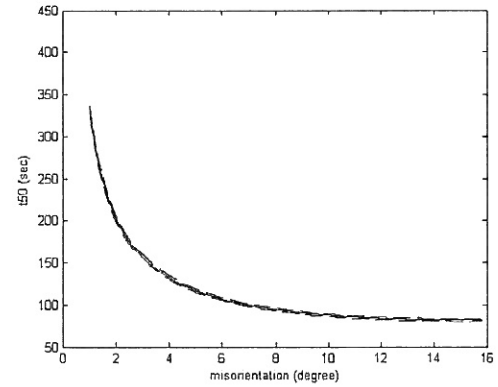


(e) $t_{50}$ sensitivity with respect to θ

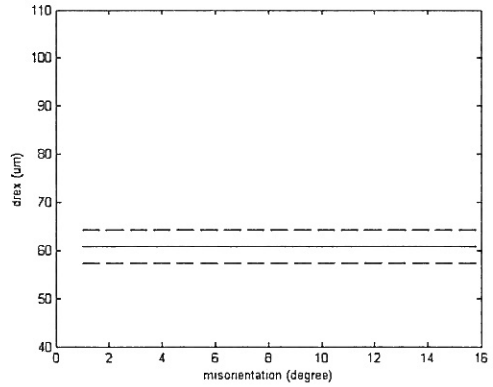


(f) $d_{rex}$ sensitivity with respect to θ

Fig. 4. Sensitivity analysis for the *p3* and *A* parameters.